Dalton Transactions

The impact of an isoreticular expansion strategy on the performance of iodine catalysts supported in multivariate zirconium and aluminum metal-organic frameworks

Journal:	*Dalton Transactions*
Manuscript ID	DT-ART-01-2019-000368.R1
Article Type:	Paper
Date Submitted by the Author:	12-Apr-2019
Complete List of Authors:	Tahmouresilerd, Babak; Texas Tech University, ; Iran University of Science and Technology, Moody, Michael; Texas Tech University Agogo, Louis; Texas Tech University Cozzolino, Anthony; Texas Tech University, Department of Chemistry and Biochemistry

Dalton Transactions

ARTICLE

The impact of an isoreticular expansion strategy on the performance of iodine catalysts supported in multivariate zirconium and aluminum metal-organic frameworks.

Received 00th January 20xx,
Accepted 00th January 20xx

DOI: 10.1039/x0xx00000x

www.rsc.org/

Babak Tahmouresilerd, Michael Moody, Louis Agogo, and Anthony F. Cozzolino*

Iodine functionalized variants of DUT-5 (Al) and UiO-67 (Zr) were prepared as expanded-pore analogues of MIL-53 (Al) and UiO-67 (Zr). They were prepared using a combination of multivariate and isorecticular expansion strategies. Multivariate MOFs with a 25% iodine-containing linker was chosen to achieve an ideal balance between a high density of catalytic sites and sufficient space for efficient diffusion. Changes to the oxidation potential of the catalyst as a result of the pore-expansion strategy led to a decrease in activity with electron rich substrates. On the other hand, these larger frameworks proved to be more efficient catalysts for substrates with higher oxidation potentials. Recyclability tests for these larger MOFs showed sustained catalytic activity over multiple recycles.

Introduction

The crystallinity, structural flexibility and tunability, thermal stability, and high surface area of metal-organic frameworks (MOFs) have led to their adoption as heterogeneous supports for catalysts.[1–5] One useful strategy for translating successful homogeneous catalysts into MOFs is to incorporate them into the organic linkers.[6–10] Reticular design strategies allow these linkers to be installed in known crystal topologies, either uniformly, or mixed with a linker of the same length to give a multivariate MOF. One of the important considerations in the choice of linker and topology is framework stability. To this end, MOFs with enhanced chemical and thermal stability are being developed.[11–13] Another critical consideration is pore and pore-aperture size. This affects the ability of substrates to diffuse through the pores and reach the catalytic site. It can also constrain the catalyst which can presumably influence the stability of transition states. To address the pore and aperture size concerns, a key strategy that has emerged is to increase the pore size by increasing the length of the organic linkers, the so-called *isoreticular expansion* strategy.[14–18] Limitations of this strategy include increased fragility of the framework and also the possibility of an interpenetrated structure. Considering that modification of a linker to include a catalytically active site usually increases the radius of the linker, and therefore decreases accessible pore volumes, an alternative strategy is to prepare multivariate MOFs where only one linker per pore (or less) contains the catalyst, thereby reducing the occupied space.[19,20]

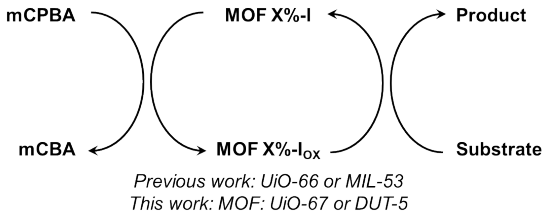

Scheme 1. Generic mechanism catalytic oxidation of aromatic diols by heterogeneous iodine catalyst in presence of mCPBA.

Hypervalent iodine has found use as an oxidant in many chemical transformations, including as facile and green reagents in organic synthesis.[21–24] Some iodine-mediated transformation can be performed catalytically with appropriate terminal oxidants.[25–28] We have recently reported a recyclable iodine catalyst supported in a metal-organic framework catalyst that was competent for the oxidation of hydroquinones using terminal oxidant metachloroperbenzoic acid (mCPBA) as depicted in Scheme 1.[29] A multivariate approach was used to maximize pore and aperture size in order to accommodate reagents and oxidants in the pores of the framework and allow for catalytic oxidation to occur within the MOF. Frameworks in which 25% of the linkers contained the catalysts showed an ideal balance between catalyst loading and catalyst accessibility. There were, however, some limitations in the catalytic performance of MOFs with respect to the yields of the reaction, the scope of substrates, the size of the substrate, and the recyclability of the catalysts. In the current study, the impact of a combination of multivariate and isoreticular expansion

Department of Chemistry and Biochemistry, Texas Tech University, Box 1061, Lubbock, Texas 79409-1061, USA. E-mail: anthony.f.cozzolino@ttu.edu; Fax: +1 806 742 1289; Tel: +1 806 834 1832Address here.

† Electronic supplementary information (ESI) available: Synthesis of MOFs, catalysis conditions, NMR spectra, summary of all reactions, or other electronic format see DOI: 10.1039/c8cy00794b

strategies on the catalytic performance of iodine supported in larger zirconium and aluminum-based MOFs is studied (Figure 1). We highlight an often-overlooked consideration with the isoreticular expansion strategy – namely that the lengthening of the linker can have unintended consequences on the electronic structure of the catalyst itself.

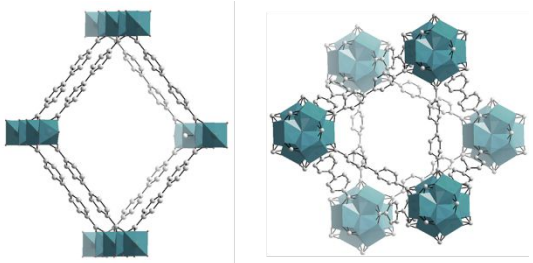

Figure 1. The depiction of DUT-5 (Al) (left),[30] and the octahedral pore in UiO-67 (Zr) (right).[31] Metal coordination spheres are represented with polyhedra. Hydrogen atoms have been removed for clarity.

Results and Discussion

Preparation and Characterization of Iodine Containing Frameworks

Iodine-containing MOFs with larger accessible inner volumes were prepared using a combination of multivariate and isoreticular expansion strategies. The iodine containing linker (H_2IBPDC) was prepared by adapting reported literature procedures as shown in Scheme 2.[32–34] The MOFs were prepared by treating the appropriate mixture of linkers with zirconium (IV) chloride or aluminum chloride hexahydrate; an adaption of literature conditions for the parent frameworks. It should be noted that the Zr frameworks (UiO-67) were prepared in the presence of HCl as a modulator to reduce or eliminate defects in the framework.[35] This yielded the multivariate UiO-67 X%-I or DUT-5 X%-I where X represents the percentage of linkers that are functionalized with I (Scheme 3).[30,36–38]

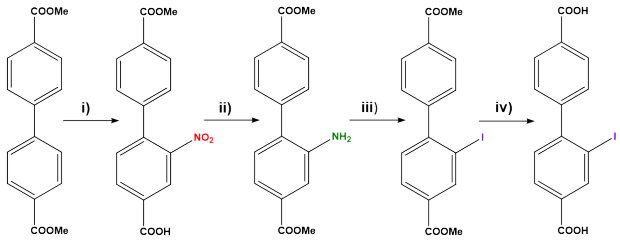

Scheme 2. Preparation of H_2IBPDC. Conditions and reagents: i) HNO_3, H_2SO_4, 0-4 °C, 5 h,[32] ii) MeOH, HCl, Sn, 80 °C,[39] iii) $NaNO_2$, HCl, 0-4 °C, NaI, 22 °C,[32] iv) KOH, THF, reflux.[34]

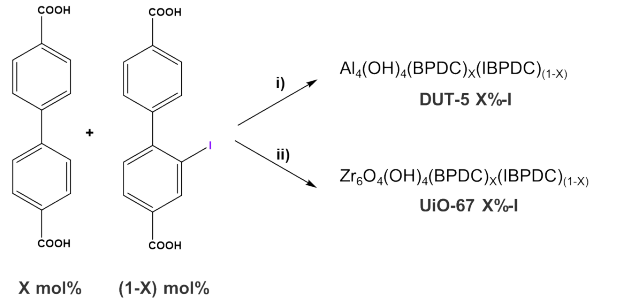

Scheme 3. Preparation of multivariate DUT-5 X%-I and UiO-67 X%-I frameworks. Conditions and reagents: i) $AlCl_3 \cdot 6H_2O$, DMF, 120 °C, 24 h,[30,36] ii) $ZrCl_4$, DMF, ultrapure water, 95 °C, 100 h.[37,38]

Powder X-ray diffraction (PXRD) analyses were performed upon isolation of the frameworks and also following activation of the frameworks. The patterns were compared with simulated patterns from the crystal structures of the parent MOFs to verify that the anticipated framework was formed and retained. All the PXRD patterns for UiO-67 X%-I and DUT-5 X%-I are in the good agreement those of UiO-67 and DUT-5 (Figure 1). [30,31]

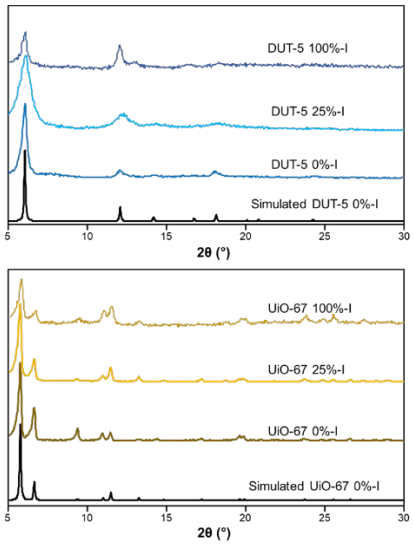

Figure 2. PXRD patterns of activated DUT-5 25%-I, DUT-5 0%-I, and simulated DUT-5 0%-I[30] (top), and UiO-67 25%-I, UiO-67 0%-I and simulated UiO-67 0%-I (bottom).[31]

Thermogravimetric analysis (TGA) was used to establish the thermal stability and the temperature limits for activation and reactions. Both activated frameworks demonstrate good stability up to 400 °C (Figure 3). These values are slightly lower than the values reported for UiO-67 0%-I[37] (500 °C) and DUT-5 0%-I[30] (430 °C). It has been previously demonstrated that multivariate DUT-5 frameworks show a decrease in stability with increasing functionalization.[36] These iodo-functionalized frameworks show roughly the same stability as the smaller analogs.[29] TGA analysis for both UiO-67 25%-I and DUT-5 25%-I after activation revealed three distinguishable profiles of weight loss. The first profile of 1% weight loss (A→B, 50-100 °C) and the second profile of additional 6% and 3% weight loss (100–400 °C) for UiO-67 25%-I and DUT-5 25%-I can be assigned

to the loss of adsorbed water. The third profile with a weight loss of 60% and 78% for UiO-67 25%-I and DUT-5 25%-I can be assigned to the thermal decomposition of the frameworks and the formation of the appropriate metal oxide, ZrO_2, and Al_2O_3, respectively.

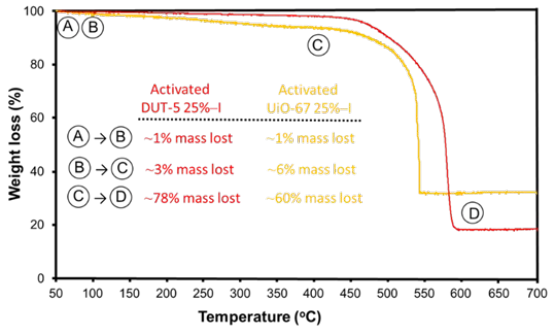

Figure 3. TGA of activated UiO-67 25%-I (yellow) and DUT-5 25%-I (red) at a ramp rate of 10 °C min^{-1} under a flow of air.

ATR-FTIR spectroscopy was performed on both UiO-67 25%-I and DUT-5 25%-I to verify the absence of impurities in the pores of the activated frameworks. In particular, DMF from the synthesis or excess neutral linker could be present. Excess unreacted ligands could leach during catalytic experiments and perform catalysis homogeneously. The spectra of the activated MOFs revealed that the bands attributed to impurities in the as-synthesized frameworks are absent, consistent with full activation of the materials (Figure 4). The spectrum for DUT-5 25%-I shows vibrational bands in the typical region for symmetric and asymmetric stretching modes (1421 cm^{-1} and 1595 cm^{-1}, respectively) of the bridging carboxylate groups which is in good agreement with the synthesized DUT-5 0%-I reported in the literature.[30] Similarly, the bands at 1404 and 1593 cm^{-1} in UiO-67 25%-I can be assigned to the symmetric and asymmetric stretching modes of the carboxylate; an excellent match with the reported bands values for UiO-67 0%-I.[40]

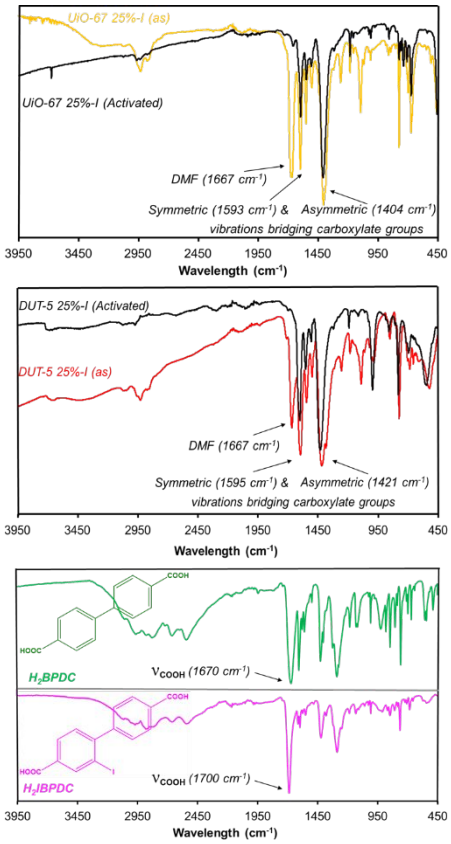

Figure 4. Di-ATR FTIR of as-synthesized and activated UiO-67 25%-I (top) and DUT-5 25%-I (middle), and linkers (bottom). All spectra plotted as attenuation.

The nitrogen adsorption-desorption measurements for activated UiO-67 25%-I and DUT-5 25%-I were conducted to establish the specific surface areas, pore size distributions, and pore volumes. Analysis of the isotherms reveals a type I isotherm for both UiO-67 25%-I and DUT-5 25%-I confirming the expected microporosity with narrow pore size distributions (Figure 5 and S8). The calculated surface area and pore volume for UiO-67 25%-I (S_{BET} = 1795 m^2/g, V_{micro} = 0.877 mL/g) and DUT-5 25%-I (S_{BET} = 1120 m^2/g, V_{micro} = 0.550 mL/g) are in a good agreement with the values reported in the literature (Table 1).[30,36–38] Nitrogen sorption for DUT-5 25%-I shows a lower surface area and pore volume than the literature value for the framework without the iodo-functionalized linker, consistent with the large iodine occupying space in the pores. The multivariate strategy prevents the large iodine from occupying a significant fraction of the pore, in line with other functionalized DUT-5 analogues. Importantly, the surface area and micropore volume for both MOFs are significantly higher than the previously reported catalysts UiO-66 25%-I and MIL-53 25%-I which should allow for more efficient diffusion of molecules within the framework. The pore size distribution analysis for UiO-67 25%-I showed two different pore sizes with diameters 1.02 nm and 1.96 nm, assigned to the tetrahedral and octahedral pores, respectively. The pore size distribution for DUT-5 25%-I indicated a major pore with a width of 1.02 nm.

Table 1. Molar Brunauer-Emmett-Teller (BET) surface areas and pore volumes for the UiO-67 (Zr) and DUT-5 (Al) obtained from nitrogen adsorption isotherms at 77 K.

MOF	BET surface area ($\times 10^3$ $m^2 \cdot mol^{-1}$)[a]	Pore volume (mL/mol)	Source
UiO-67 0%-I	771	469	[41]
UiO-67 25%-I	690	334	This work
UiO-67 100%-I	171	113	This work
DUT-5 0%-I	567	193	[30]
DUT-5 25%-I	354	174	This work
DUT-5 100%-I	317	153	This work

a) Based on idealized formula $[Zr_6O_4(OH)_4(L)_6]$ for UiO-67 and $[Al_4(OH)_4(L)_4]$ for DUT-5, normalized to one Zr or Al, respectively

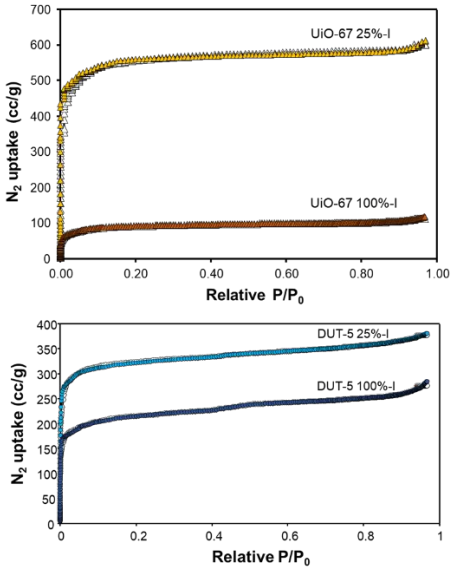

Figure 5. Nitrogen sorption isotherm (filled triangles or circles absorption, open triangles or circles desorption) of UiO-67 25 and 100%-I (top) and DUT-5 25 and 100%-I (bottom) (77 K).

The ratio of iodo-functionalized linker to unsubstituted linker was verified through NMR analysis of the digested frameworks. For both frameworks, the anticipated ratio of linkers, based on reaction stoichiometry, was approximately observed (28%-I in UiO-67 25%-I and 21% for DUT-5 25%-I, see Figures S6 and S7). It is conceivable that the material is a mixture of two pure-phase MOFs containing either 0% $IBPDC^{2-}$ or 100% $IBPDC^{2-}$. To ensure the even distribution of iodo-functionalized linker in the frameworks, energy-dispersive X-ray spectroscopy (EDS) analyses were performed. EDS–mapping results for activated UiO-67 25%-I and DUT-5 25%-I particles coated with Au/Pd confirm that the iodo-functionalized linker is consistently distributed throughout both frameworks (Figure 6).

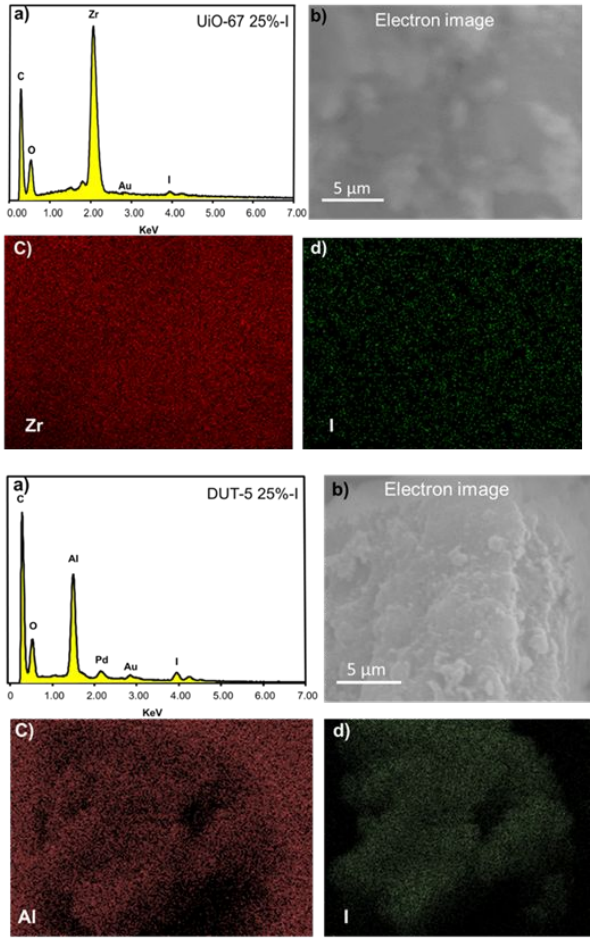

Figure 6. Top, a) EDS spectrum of UiO-67 25%-I, b) SEM image, and c, d) EDS–mapping results for Zr and I over UiO-67 25%-I particles coated with Au/Pd after activation, bottom, a) EDS spectrum of DUT-5 25%-I, b) SEM image, and c, d) EDS–mapping results for Zr and I over DUT-5 25%-I particles coated with Au/Pd after activation.

Catalytic Evaluation

The catalytic oxidation of hydroquinone to benzoquinone (Scheme 4) was chosen as a model reaction to evaluate the performance of these larger frameworks. Catalysis was performed in nitromethane with 2.9 eq. (mCPBA) as co-oxidant, 20 mol% I catalyst, 60 min and 50 °C. mCPBA was chosen as it is well-established as a suitable terminal oxidant for catalytic oxidations with iodine.[42,43] MOFs with 0% (the same number of moles of MOF were used as with 25%-I), 25% and 100% iodine functionalized ligands were tested against these conditions. Almost no difference was observed (Table 2, entry 1) in the yield of the reaction from the two control conditions (no MOF and MOF with no I), indicating that the framework itself is inactive and that iodine is necessary for catalysis to occur. UiO-67 25%-I and DUT-5 25%-I were the most competent catalysts for the oxidation of hydroquinone to benzoquinone with 75% and 73% yield (Table 2, entry 1), respectively, beyond the background reaction without MOF (8%). Consistent with expectation, MOFs with 100% I functionalized linker performed worse than those with 25% iodine functionalized linker. This behaviour aligns with the smaller pore volumes in the MOFs with higher iodine loading (Table 1). Notably, this effect is not as dramatic as it was

with the smaller MOFs, UiO-66 and MiL-53.[29] Similarly higher yields were observed in acetonitrile for the MOFs with 25% iodine-containing linker. With the much larger substrate, 2,5-di-tert-butylhydroquinone, higher yields were again observed in the frameworks with less iodine per pore. Due to the superior performance, UiO-67 25%-I and DUT-5 25%-I were used for subsequent reactions. A split test was performed with both iodo-functionalized MOFs to verify that catalysis occurs heterogeneously, rather than as a result of catalyst leaching. After the separation of catalyst from the reaction mixture, no additional conversion was observed (Figure S14), confirming heterogeneous catalysis.

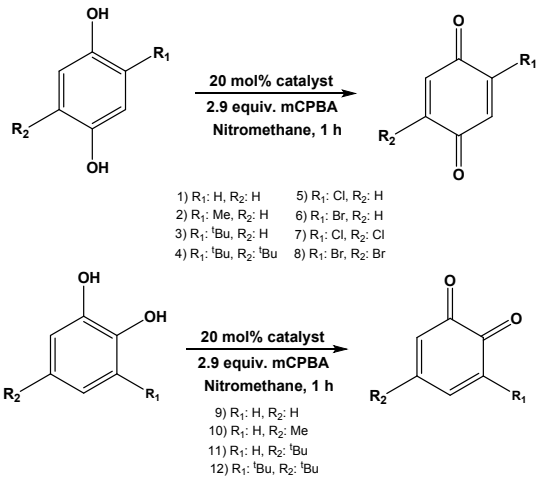

Scheme 4. The oxidation of aromatic diols shown with typical catalytic conditions.

Table 2. The yield of catalytic oxidation of hydroquinone and catechol derivatives with iodo-functionalized MOFs.[a]

#	Product	Temp. (°C)	Yield (%)[a, b] DUT-5 25%-I	UiO-67 25%-I	Background[d]
1		24	19 (22)	33 (36)	3
		50	0 (8) [c]	0 (8)[c]	8
		50	73 (81)	75 (83)	8
2		24	21 (50)	25 (54)	29
3		24	8 (39)	11 (42)	31
4		24	29 (70)	24 (65)	41
5		50	72 (96)	52 (76)	24
6		50	85 (92)	73 (80)	7
7		50	90 (97)	79 (86)	7
8		50	89 (94)	77 (82)	5
9		24	13 (13)	48 (48)	0
		50	42 (42)	56 (56)	0
10		24	26 (47)	41 (62)	21
11		24	58 (63)	85 (90)	5
12		24	29 (79)	27 (77)	50

a) Values were determined by ^{1}H NMR using methylsulfonylmethane (MSM) as an internal standard.

b) The yield of reaction beyond the background reaction is provided, the total yield is in parentheses.

c) Performed with UiO-67 0%-I or DUT-5 0%-I.

d) Direct oxidation of substrate with mCPBA

The effect of catalyst loading (5, 10, and 20 mol%) on the oxidation of hydroquinone under the conditions listed in Scheme 4 was studied. The turnover numbers (TONs) for the yields beyond the background reactions are provided in Figure 7. The TONs at the lowest loadings are 5 and 10 for DUT-5 25%-I and UiO-67 25%-I, respectively. This indicates that UiO-67 is a faster catalyst. As the loading is increased to 10%, no change is observed for DUT-5 25%-I, however a decrease in TON is observed for UiO-67 25%-I. The yield of the reaction does not change for UiO-67 25%-I upon further doubling of the catalyst loading suggesting that the reaction has slowed significantly. A similar decrease in TON is observed upon increasing the loading

of DUT-5 25%-I to 20 mol%. The slowing of the reaction can be, in part, attributed to the decrease in the concentration of the substrate. An additional factor that was suggested by Harned for homogeneous systems is that the concentration of metachlorobenzoic acid is increasing. This, in turn can allow for the metachlorobenzoate to functionalize the hypervalent iodine.[43] While this is presumed to be beneficial with homogeneous catalysts, the presence of two metachlorobenzoate groups on the iodine in the MOF could readily block access to the pores or even the catalyst itself. Two possible remedies for this would be to utilize flow chemistry in order to reduce the build-up of the organic acid byproduct and/or to find a suitable alternative terminal oxidant that is smaller such as peracetic acid.

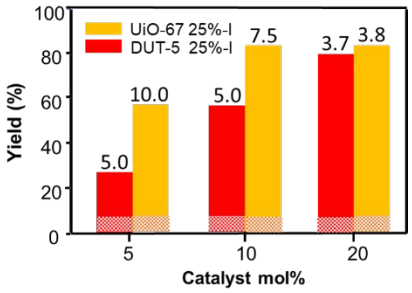

Figure 7. The effect of different catalyst loading (5, 10, and 20 mol%) on the yield of quinone for UiO-67 25%-I and DUT-5 25%-I. Shaded areas show extent of background reaction, TONs beyond background presented at the top of each column.

In the case of UiO-67 25%-I, a yield of 33% and 75% was observed for the oxidation of hydroquinone at 24 °C and 50 °C, respectively. These values are roughly the same as the yields obtained with UiO-66 25%-I under similar conditions. Due to the larger pore size in UiO-67 25%-I, an increase in the yield of the reaction was expected; however, a slight decrease in yield for the catalytic oxidation of hydroquinone was observed. To rationalize this behaviour, the effect of the linker elongation strategy on the catalytic site itself was investigated. The oxidation potential of both linkers (BDC^{2-} and $BPDC^{2-}$) was evaluated homogeneously using the methyl esters of the two linkers, Me_2IBPDC and Me_2IBDC, as model systems. Cyclic voltammetry revealed that the shorter linker is more readily oxidized by 0.2 V (see Figure 8). This contrasts with the DFT calculated energies of the HOMOs, iodine lone pairs, which are the same in both molecules within 0.04 eV (see Tables S7 and S8). One reason for the difference in the experimentally determined oxidation potential is the ability of the ester oxygen to engage in an intramolecular halogen bond with the oxidized iodine,[44] thus stabilizing the higher oxidation state. This is only possible in the shorter linker where the iodine is ortho to the ester. In the MOFs, the same interaction would occur with the carboxylate groups that are bound to the metals (See Figure 9). Examples of this behaviour are observed with a variety of hypervalent iodine systems with neighbouring nucleophilic sites.[45–48] As a result, the catalyst in the larger pore framework is less readily oxidized and therefore, less efficient even though there is more space. This effect is not observed with MIL-53/DUT-5 as the increase in accessible space appears to offset the change to the catalytic site. Using DUT-5 25%-I for oxidation of hydroquinone at 24 and 50 °C, a yield of 19 and 73% were observed when compared to the MIL-53 25%-I (10 and 37%).

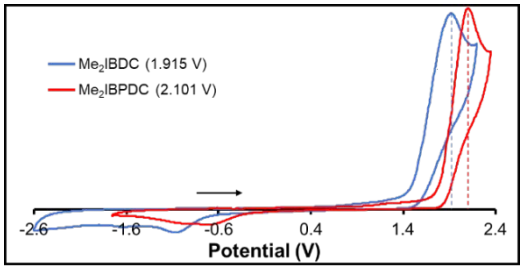

Figure 8. Cyclic Voltammogram (CV) of dimethyl 2-iodoterephthalate and dimethyl 2-iodo-[1,1'-biphenyl]-4,4'-dicarboxylate in acetonitrile in 0.1 M Bu_4NBF_4. At 100 mV/s vs. Fc/Fc^+.

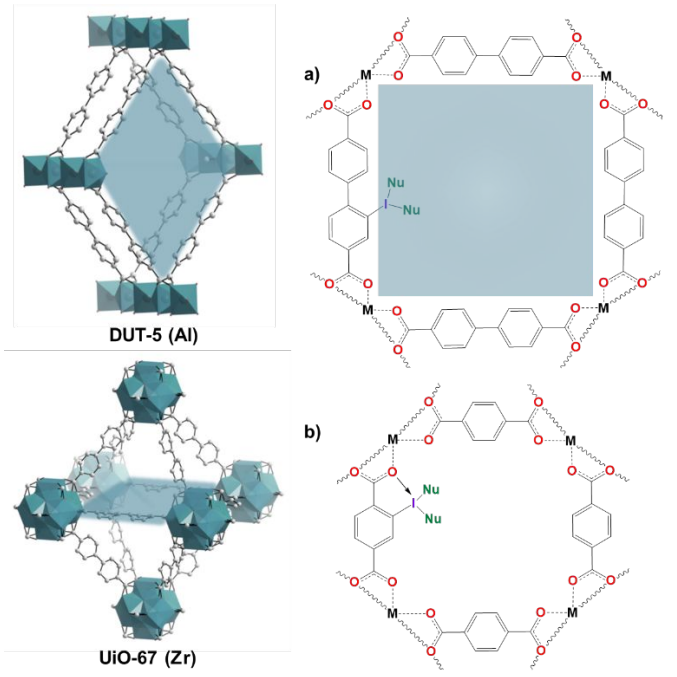

Figure 9. Proposed *in situ* generated hypervalent iodine(III) supported by nucleophile Nu^- in the pores (highlighted in blue for DUT-5 and UiO-67) of a) DUT-5 25%-I or UiO-67 25%-I or b) MIL-53 25%-I or UiO-66 25%-I.

Despite having good catalytic performance, UiO-66 25%-I was not able to be recycled with retained activity towards the oxidation of hydroquinone.[29] With the larger UiO-67 25%-I, however, the catalytic conversion remained constant over four runs (Figure 10, top). In the case of DUT-5 25%-I, for the first and second runs, a conversion of 85% was observed. For the third and fourth runs, the catalytic conversion dropped to 84% and 82%, respectively. This small loss in conversion for the third and the fourth run are attributed to catalyst attrition from manipulations between recycles. This series of conversions for DUT-5 25%-I shows improvement when compared to the same family of MOF with the smaller linker (Figure 10, bottom).[29] PXRD patterns for the catalysts after the first and fourth runs were obtained and both frameworks retain their crystallinity (Figure 11). SEM images of UiO-67 25%-I before catalysis and

after the fourth run reveal that the overall sizes and shapes of the crystallites are retained, but there appears to be selective etching of the crystallites which leads to broader peaks in the PXRD. This may have the added benefit of allowing substrates and oxidants to more readily move into the pores of the MOF. In the smaller MOFs, restricted access to the catalyst as a result of accumulation of organic groups bound to the hypervalent iodine species may be a limiting factor in the ability to recycle the frameworks. With the larger frameworks, this appears to be overcome.

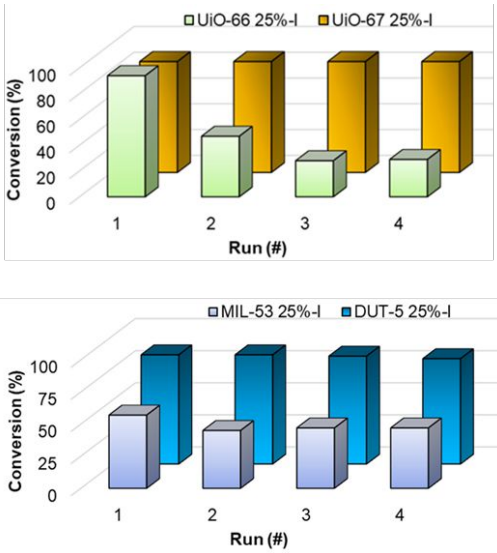

Figure 10. Catalyst recyclability for oxidation of hydroquinone to benzoquinone in the presence of UiO-67 25%-I compared to UiO-66 25%-I (top),[29] and DUT-5 25%-I compared to MIL-53 25%-I (bottom).[29] Conditions: 1 h, 20 mol% catalyst, 2.9 eq. mCPBA, nitromethane, 50 °C. Values were determined by ^{1}H NMR in the presence of MSM as an internal standard.

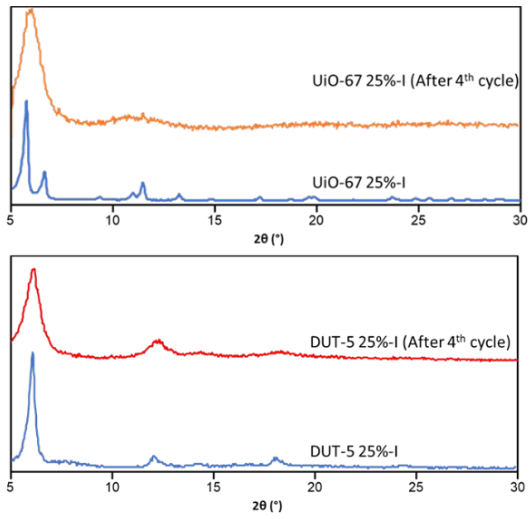

Figure 11. PXRD patterns of UiO-67 25%-I before the catalytic reaction, and the fourth run.

The choice of solvent can play a significant role in mediating these oxidation reactions. Nitromethane was previously found to promote both high reactivity and selectivity with the smaller frameworks.[29] Halogenated solvents were not previously tested with the smaller MOFs, but it has been shown that they can accelerate the yield of catalytic reactions with hypervalent iodine.[49] The catalytic oxidation of hydroquinone to quinone was examined over 1 h in the presence of ethyl alcohol or 2,2,2-trifluoroethanol (TFE) under typical catalytic conditions. With ethyl alcohol as a solvent, a yield of 12% was observed over 1 h. The yield of catalytic reaction in the presence of TEF reached 61% after just 10 minutes, but the reaction proceeded sluggishly after that. PXRD following the reaction revealed that the crystallinity of the UiO-67 25% had been drastically reduced.

Evaluation of Other Substrates

The scope of the substrates was expanded to other aromatic diols. The first set of para-hydroquinone substrates increase in size through the incorporation of electron rich alkyl groups (Table 2, entries 1-4). Based on size estimates from MM2 optimized structures, all of the substrates have a minimum diameter orientation that should allow them to fit into DUT-5 (pore apertures of ~11 Å). UiO-67 has smaller pore apertures (~7 Å, see Figure S16) which may prohibit many of the larger substrates from entering the pores (See Figure S15). These more electron-rich substrates react readily with mCPBA at 50 °C, so a lower temperature was used to evaluate the catalytic activity. At 24 °C, the observed trend was an increase in the yield of the background reaction, from 3% for p-hydroquinone to 41% for 2,5-di-tert-butylhydroquinone. This increase in background reactivity mirrors the decrease in oxidation potential characterized by cyclic voltammetry (Figure 12a, 0.97 eV to 0.84 eV). A comparison with the average calculated bond dissociation free energies (BDFEs)[50] mirrors this trend. In fact, there is a strong correlation between the experimental oxidation potentials measured here and the reported BDFEs.[50] In the presence of the catalyst, a similar trend in the reaction yield was not observed. For DUT-5, a yield beyond the background reaction was observed in all cases, but the yield was not proportional to the increase in background reactivity. In other words, enhanced activity was not observed for more easily oxidized substrates. This is consistent with the larger substrates not diffusing into the pores as readily. This is more pronounced with UiO-67 25%-I which has a more restricted pore aperture. In addition to this, the direct reaction of mCPBA with the substrate is sufficiently favorable given that higher oxidation potential of the catalyst and the lower oxidation potentials of these substrates that the catalytic reaction may be hampered under these conditions. This is consistent with the catalytic activity observed with the more readily oxidized UiO-66 25%-I.[29]

Hydroquinone derivatives containing electron withdrawing groups (Table 2, entries 5-8) were probed. The chlorinated and brominated derivatives have a similar size profile to the methyl substituted hydroquinone but are not as readily oxidized (Figure 12b). With these substrates, a high yield of reaction beyond the background reaction was observed at 50 °C. The yields of the catalytic reactions for oxidation of chlorohydroquinone and 2,5-dibromohydroquinone (Table 2, entries 5, 8) were reported to be 40 and 67% for UiO-66 25%-I and 20 and 10% for MIL-53 25%-I.[29] For both substrates, the larger-pore catalysts proved to

be more efficient catalysts. This enhanced performance is attributed to the increase in pore size associated with the larger MOFs. Additional substrates 2-bromohydroquinone and 2,5-dichlorohydroquinone (Table 2, entries 6 & 7) were tested with all four catalysts. In the presence of the smaller MOFs (Table S10), the yields were significantly lower than with the larger frameworks. This is, again, consistent with the combination of larger pores and a catalyst that is a more potent oxidant.

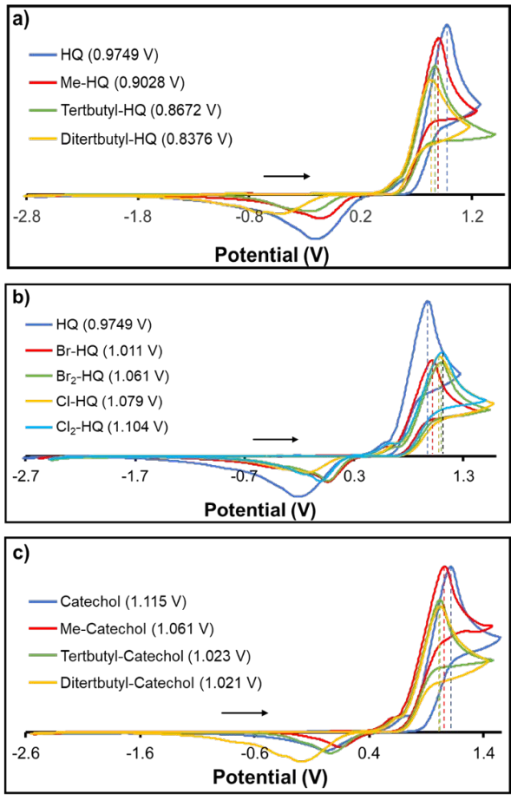

Figure 12. CVs of a) hydroquinone and hydroquinone derivatives containing electron donation groups, b) hydroquinone derivatives containing electron withdrawing groups, c) catechol and catechol derivatives containing electron donation groups. All obtained in acetonitrile in 0.1 M Bu_4NPF_6 at 100 mV/s vs. Fc/Fc^+.

Given the success of these extended frameworks with substrates that have higher oxidation potentials the substrate scope was expanded to include catechol. Catechol itself has an oxidation potential 0.14 V higher than hydroquinone and a BDFE that is calculated to be 16 kJ/mol higher than hydroquinone.[50] This increase in oxidation potential leads to a low yield of the desired product with the smaller MOFs, MIL-53 25%-I or UiO-66 25%I (6-7%, see Table S10), at 50 °C. The oxidation of catechol, 4-methylcatechol, 4-tert-butylcatechol, and 2,5-di-tert-butylhydroquinone at 24 °C using DUT-5 25%-I (Table 2, entries 9-12) gave the yields of 13%, 26%, 58%, and 29%. The same reactions with UiO-67 25%-I as the catalyst gave yields of 48%, 41%, 85%, and 27%, demonstrating that these larger MOFs can accommodate larger and more difficult to oxidize substrates. Notably, the yields appear to drop off with the most readily oxidized substrate, 2,5-di-tert-butylhydroquinone. This can be attributed to the larger size of the substrate (minimum diameter of ~9.4 Å, See Figure S15) having a limiting effect on diffusion into the pores. Consistent with expectations, raising the reaction temperature for the oxidation of catechol from 24 to 50 °C improved the yields with both frameworks.

Selectivity was evaluated by contrasting the total yield of the desired product with the overall conversion. In addition to higher yields, these isoreticularly expanded MOF catalysts lead to higher selectivities for the desired products (Table S10) in the reactions with the hydroquinones. For hydroquinone, the other observed products of oxidation include 2,5-dihydroxy-1,4-benzoquinone and maleic acid, representing an over-oxidation of hydroquinone (Figures S9 and S11).[29,51] In the absence of MOF, these side-produces account for 47% of the reaction products. This number is reduced to less than 5% in the presence of either UiO-67 25%-I or DUT-5 25%-I. Interestingly, in the presence of the UiO-67 or DUT-5 with 0% I, the selectivities were nearly identical to those without any framework. This indicates that the simple presence of the framework is not sufficient to induce selectivity. The MOFs with 100%-I have selectivities between those of the controls and the frameworks with 25%-I. Given the limited accessibility of the pores in the MOFs with 100%-I linkers, a possibility is that the observed oxidations are limited to the surface. This would imply that it is the catalytic sites within the framework that are responsible for the observed enhancement of selectivity. In further support of this, a reaction run with an esterified version the linker, under otherwise identical conditions, gave a yield of 38% (30% above background) for the desired product. The total conversion, however, was 58%, so side products account for 34% of the product mixture. While this is lower than the percentage observed with just mCPBA, it represents a much less selective reaction than is observed with the MOFs containing 25% iodine. The larger electron-rich substrates, such as 3,5-di-tert-butylcatechol and 2,5-di-tert-butylhydroquinone, have low selectivities in the MOFs with 25% I which is likely due to their inability to readily diffuse into the pores. This contrasts with the high yields and selectivities for the electron-poor hydroquinones and catechols that were studied. The precise origin of the selectivity observed in these MOFs is not known and represents an interesting line of future inquiry. Given the poorer selectivities of the homogeneous analogues, one possible model that can be used to rationalize this behaviour is that the site isolation of the catalyst in the framework prevents the formation of small amounts of bimolecular catalytically active species, such as μ-oxo-bridged hypervalent iodine molecules, which are known to be potent oxidants.[52,53]

Conclusions

Two new expanded-pore iodine-functionalized robust frameworks, based on DUT-5 (Al) and UiO-67 (Zr), were prepared as oxidization catalysts. Their performance was inferior to the analogous smaller-pore MOFs with electron-rich substrates. This resulted from an unintended change to the electronic structure as a result of the pore-expansion strategy and should serve as a cautionary note for linker elongation as a blanket strategy for creating more void volume in a MOF. This

slightly poorer performance was offset by greater stability towards recycling of the catalyst. With substrates that were more difficult to oxidize, the expanded-pore frameworks were superior catalysts as compared to their smaller analogues. This is likely a result of the combination of more space for diffusion within the framework and the higher oxidation potential of the iodine catalysts. In some cases, there was higher selectivity associated with the MOF 25%-I catalysts than in the uncatalyzed reaction of even the reaction with an analogous homogeneous catalyst.

Conflicts of Interest

There are no conflicts to declare.

Acknowledgements

The present work was support by Texas Tech University and the National Science Foundation (NMR instrument grant CHE-1048553). We are grateful for assistance from the Hope-Weeks group at Texas Tech for assistance with TGA measurements.

References

1 A. Dhakshinamoorthy, Z. Li and H. Garcia, *Chem. Soc. Rev.*, 2018, **47**, 8134–8172.
2 A. Corma, H. García and F. X. Llabrés i Xamena, *Chem. Rev.*, 2010, **110**, 4606–4655.
3 J. Gascon, A. Corma, F. Kapteijn and F. X. Llabrés i Xamena, *ACS Catal.*, 2014, **4**, 361–378.
4 J. Lee, O. K. Farha, J. Roberts, K. A. Scheidt, S. T. Nguyen and J. T. Hupp, *Chem. Soc. Rev.*, 2009, **38**, 1450–1459.
5 D. Farrusseng, S. Aguado and C. Pinel, *Angew. Chem. Int. Ed.*, 2009, **48**, 7502–7513.
6 D. Saha, R. Sen, T. Maity and S. Koner, *Langmuir*, 2013, **29**, 3140–3151.
7 S. A. Burgess, A. Kassie, S. A. Baranowski, K. J. Fritzsching, K. Schmidt-Rohr, C. M. Brown and C. R. Wade, *J. Am. Chem. Soc.*, 2016, **138**, 1780–1783.
8 B. R. Reiner, A. A. Kassie and C. R. Wade, *Dalton Trans.*, , DOI:10.1039/C8DT03801E.
9 C.-D. Wu, A. Hu, L. Zhang and W. Lin, *J. Am. Chem. Soc.*, 2005, **127**, 8940–8941.
10 S. M. Cohen, Z. Zhang and J. A. Boissonnault, *Inorg. Chem.*, 2016, **55**, 7281–7290.
11 S. Yuan, L. Feng, K. Wang, J. Pang, M. Bosch, C. Lollar, Y. Sun, J. Qin, X. Yang, P. Zhang, Q. Wang, L. Zou, Y. Zhang, L. Zhang, Y. Fang, J. Li and H.-C. Zhou, *Adv. Mater.*, 2018, **30**, 1704303.
12 Y. Bai, Y. Dou, L.-H. Xie, W. Rutledge, J.-R. Li and H.-C. Zhou, *Chem. Soc. Rev.*, 2016, **45**, 2327–2367.
13 M. Bosch, M. Zhang and H.-C. Zhou, *Adv. Chem.*, 2014, **2014**, e182327.
14 M. Eddaoudi, J. Kim, N. Rosi, D. Vodak, J. Wachter, M. O'Keeffe and O. M. Yaghi, *Science*, 2002, **295**, 469–472.
15 S. J. Garibay and S. M. Cohen, *Chem. Commun.*, 2010, **46**, 7700–7702.
16 V. Guillerm, F. Ragon, M. Dan-Hardi, T. Devic, M. Vishnuvarthan, B. Campo, A. Vimont, G. Clet, Q. Yang, G. Maurin, G. Férey, A. Vittadini, S. Gross and C. Serre, *Angew. Chem. Int. Ed.*, 2012, **51**, 9267–9271.
17 L. Ma, J. M. Falkowski, C. Abney and W. Lin, *Nat. Chem.*, 2010, **2**, 838–846.
18 H. Furukawa, N. Ko, Y. B. Go, N. Aratani, S. B. Choi, E. Choi, A. Ö. Yazaydin, R. Q. Snurr, M. O'Keeffe, J. Kim and O. M. Yaghi, *Science*, 2010, **329**, 424–428.
19 H. Fei and S. M. Cohen, *Chem. Commun.*, 2014, **50**, 4810–4812.
20 R. Sun, B. Liu, B.-G. Li and S. Jie, *ChemCatChem*, 2016, **8**, 3261–3271.
21 T. Kitamura and Y. Fujiwara, *Org. Prep. Proced. Int.*, 1997, **29**, 409–458.
22 Viktor V. Zhdankin, *Chemistry of Hypervalent Compounds*, John Wiley & Sons, Ltd, 2013.
23 V. V. Zhdankin and P. J. Stang, *Chem. Rev.*, 2008, **108**, 5299–5358.
24 E. A. Merritt and B. Olofsson, *Angew. Chem. Int. Ed.*, 2009, **48**, 9052–9070.
25 R. Bikshapathi, P. S. Prathima and V. J. Rao, *New J. Chem.*, 2016, **40**, 10300–10304.
26 R. Mu, Z. Liu, Z. Yang, Z. Liu, L. Wu and Z.-L. Liu, *Adv. Synth. Catal.*, 2005, **347**, 1333–1336.
27 M. S. Yusubov and V. V. Zhdankin, *Resour.-Effic. Technol.*, 2015, **1**, 49–67.
28 R. D. Richardson and T. Wirth, *Angew. Chem. Int. Ed.*, 2006, **45**, 4402–4404.
29 B. Tahmouresilerd, P. J. Larson, D. K. Unruh and A. F. Cozzolino, *Catal. Sci. Technol.*, 2018, **8**, 4349–4357.
30 I. Senkovska, F. Hoffmann, M. Fröba, J. Getzschmann, W. Böhlmann and S. Kaskel, *Microporous Mesoporous Mater.*, 2009, **122**, 93–98.
31 Nakeun Ko, Jisu Hong, Siyoung Sung, Kyle E. Cordova, Hye Jeong Park and Jaheon Kim, *Dalton Trans.*, 2015, **44**, 2047–2051.
32 Vyacheslav K., Dmitrii A. Vasilevskii, Andrei A. Pap, Galina V. Kalechyts, Yurii V. Matveienko, Andrei G. Baran, Nikolay A. Halinouski and Vitalii G. Petushok, *ARKIVOC*, 2008, **2008**, 69–93.
33 K. A. McDonald, N. Ko, K. Noh, J. C. Bennion, J. Kim and A. J. Matzger, *Chem. Commun.*, 2017, **53**, 7808–7811.
34 R. K. Deshpande, J. L. Minnaar and S. G. Telfer, *Angew. Chem. Int. Ed.*, 2010, **49**, 4598–4602.
35 O. V. Gutov, M. G. Hevia, E. C. Escudero-Adán and A. Shafir, *Inorg. Chem.*, 2015, **54**, 8396–8400.
36 M. A. Gotthardt, S. Grosjean, T. S. Brunner, J. Kotzel, A. M. Gänzler, S. Wolf, S. Bräse and W. Kleist, *Dalton Trans.*, 2015, **44**, 16802–16809.
37 S. Chavan, J. G. Vitillo, D. Gianolio, O. Zavorotynska, B. Civalleri, S. Jakobsen, M. H. Nilsen, L. Valenzano, C. Lamberti, K. P. Lillerud and S. Bordiga, *Phys. Chem. Chem. Phys.*, 2012, **14**, 1614–1626.
38 M. J. Katz, Z. J. Brown, Y. J. Colón, P. W. Siu, K. A. Scheidt, R. Q. Snurr, J. T. Hupp and O. K. Farha, *Chem. Commun.*, 2013, **49**, 9449–9451.
39 R. K. Deshpande, J. L. Minnaar and S. G. Telfer, *Angew. Chem. Int. Ed.*, 2010, **49**, 4598–4602.
40 J. H. Cavka, S. Jakobsen, U. Olsbye, N. Guillou, C. Lamberti, S. Bordiga and K. P. Lillerud, *J. Am. Chem. Soc.*, 2008, **130**, 13850–13851.
39 E. Langseth, O. Swang, B. Arstad, A. Lind, J. H. Cavka, T. L. Jensen, T. E. Kristensen, J. Moxnes, E. Unneberg and R. H. Heyn, *Mater. Chem. Phys.*, 2019, **226**, 220-225.
42 T. Dohi and Y. Kita, *Chem. Commun.*, 2009, 2073–2085.
43 A. M. Harned, *Tetrahedron Lett.*, 2014, **55**, 4681–4689.
44 F. Heinen, E. Engelage, A. Dreger, R. Weiss and S. M. Huber, *Angew. Chem. Int. Ed.*, 2018, **57**, 3830–3833.
45 D. Macikenas, E. Skrzypczak-Jankun and J. D. Protasiewicz, *Angew. Chem. Int. Ed.*, 2000, **39**, 2007–2010.
46 B. V. Meprathu, M. W. Justik and J. D. Protasiewicz, *Tetrahedron Lett.*, 2005, **46**, 5187–5190.

47 V. V. Zhdankin, A. Y. Koposov, B. C. Netzel, N. V. Yashin, B. P. Rempel, M. J. Ferguson and R. R. Tykwinski, *Angew. Chem. Int. Ed.*, 2003, **42**, 2194–2196.
48 V. V. Zhdankin, A. Y. Koposov, D. N. Litvinov, M. J. Ferguson, R. McDonald, T. Luu and R. R. Tykwinski, *J. Org. Chem.*, 2005, **70**, 6484–6491.
49 T. Yakura, Y. Tian, Y. Yamauchi, M. Omoto and T. Konishi, *Chem. Pharm. Bull. (Tokyo)*, 2009, **57**, 252–256.
50 X.-Q. Zhu, C.-H. Wang and H. Liang, *J. Org. Chem.*, 2010, **75**, 7240–7257.
51 E. Guibal, T. Vincent, E. Touraud, S. Colombo and A. Ferguson, *J. Appl. Polym. Sci.*, 2006, **100**, 3034–3043.
52 T. Dohi, T. Nakae, N. Takenaga, T. Uchiyama, K. Fukushima, H. Fujioka and Y. Kita, *Synthesis*, 2012, **44**, 1183–1189.
53 T. Dohi, N. Takenaga, K. Fukushima, T. Uchiyama, D. Kato, S. Motoo, H. Fujioka and Y. Kita, *Chem. Commun.*, 2010, **46**, 7697–7699.

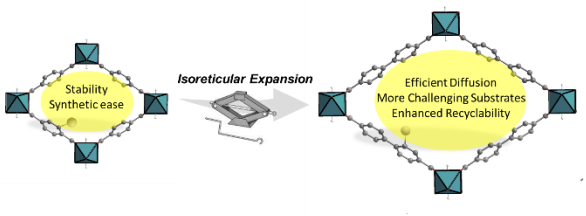

A new iodine catalyst was supported in two different MOFs and the catalytic activity for the oxidation of hydroquinones and catechols was evaluated.